Highly rectifying p-$ZnCo_2O_4$/n-ZnO heterojunction diodes

Friedrich-Leonhard Schein, Markus Winter, Tammo Böntgen, Holger von Wenckstern, and Marius Grundmann

Citation: Appl. Phys. Lett. **104**, 022104 (2014); doi: 10.1063/1.4861648
View online: https://doi.org/10.1063/1.4861648
View Table of Contents: http://aip.scitation.org/toc/apl/104/2
Published by the American Institute of Physics

Highly rectifying p-$ZnCo_2O_4$/n-ZnO heterojunction diodes

Friedrich-Leonhard Schein,[a] Markus Winter, Tammo Böntgen,[b] Holger von Wenckstern, and Marius Grundmann
Universität Leipzig, Fakultät für Physik und Geowissenschaften, Institut für Experimentelle Physik II, Linnéstraße 5, 04103 Leipzig, Germany

(Received 28 November 2013; accepted 24 December 2013; published online 14 January 2014)

We present oxide bipolar heterojunction diodes consisting of p-type $ZnCo_2O_4$ and n-type ZnO fabricated by pulsed-laser deposition. Hole conduction of $ZnCo_2O_4$ (ZCO) was evaluated by Hall and Seebeck effect as well as scanning capacitance spectroscopy. Both, ZCO/ZnO and ZnO/ZCO type heterostructures, showed diode characteristics. For amorphous ZCO deposited at room temperature on epitaxial ZnO/Al_2O_3 thin films, we achieved current rectification ratios up to 2×10^{10}, ideality factors around 2, and long-term stability. © *2014 AIP Publishing LLC*.
[http://dx.doi.org/10.1063/1.4861648]

In the past years, the scientific interest in wide bandgap oxide semiconductors has increased tremendously. This emerging field is driven by various functionalities such as piezoelectricity, magnetism (or multiferroic behavior if combined), or simply transparency that cannot be satisfyingly realized using conventional semiconductors.[1,2] However, fundamental differences between established materials such as Si or GaAs, even GaN, and oxide semiconductors exist. One major aspect is that bipolar doping becomes more and more unlikely with increasing bandgap. In principle, transparent semiconducting oxides (TSOs) are unipolar and do not allow realization of pn-homodiodes. This is aggravated by the fact that most TSOs are naturally n-type, thus only few p-TSOs like NiO[3] (binaries), $CuAlO_2$[4] (delafossites), or $ZnCo_2O_4$ (ZCO)[5] (spinels) are at choice to realize oxide pn-heterojunctions.

The latter material class of zinc spinels ZnM_2O_4 (M = Co, Rh, Ir) has gained much interest since Mizoguchi *et al.*[6] reported $ZnRh_2O_4$ as p-TSO. Much attention is due to the exceptional preservation of p-type conductivity even in the amorphous state. These materials are also used as prototypes to understand doping rules in ternary oxides where Zn on octahedral M place was found to be an acceptor.[7–9] Promising devices like amorphous all-oxide diodes using $ZnRh_2O_4$ or $ZnCo_2O_4$ as p-type layer were reported.[5,10] Recently, we presented ZCO/ZnO junction field-effect transistors.[11,12] Here, we report on the exceptionally high rectification and long-term stability of p-ZCO/n-ZnO heterojunction diodes.

The ZCO target for pulsed-laser deposition (PLD) was made from Co_3O_4 and ZnO powders which were mixed, milled, and then pressed into a cylindrical pellet with a diameter of 25 mm. A first sintering process at 1000 °C for 6 h in ambient air gave insufficient target solidity. Thus, a second sintering process at 1200 °C for 6 h was applied. Energy dispersive X-ray spectroscopy measurements revealed a ratio of atomic percent of Zn/(Zn + Co) of 0.27 in the target and 0.37–0.41 in the films but deviations of 5 at. % and more are possible. However, the powder weight ratio $m(\mathrm{ZnO})/(m(\mathrm{ZnO}) + m(\mathrm{Co_3O_4}))$ was 0.4, so we expect a slightly Zn-rich composition

We then fabricated ZCO sample series with varying growth temperature T_G and oxygen partial pressure $p(O_2)$ on *a*-sapphire substrates. We found a growth parameter window of $p(O_2) = 0.016 - 0.05$ millibar and T_G up to ≈460 °C to obtain samples having electrical conductivity in the range of $\sigma = 1$–20 S/cm. Room-temperature deposited ZCO films showed no reflexes in XRD measurements. Also Raman spectroscopy did not reveal distinct peaks but only a broad band in the spectral region of the Raman active phonon modes. Thus, we conclude that these films are amorphous. Films fabricated at higher T_G exhibited (111)-orientation and the evolution of a ZnO phase for $T_G \gtrsim 500$ °C (not shown). Hall effect measurements on the ZCO films turned out to be difficult, and we often observed a fluctuating sign of the Hall coefficient R_H. A low hole mobility—reported values are mostly below 0.4 $cm^2/(Vs)$ (Refs. 5, 8, 13, and 14)—hampers reliable Hall effect data. However, for some samples fabricated at T_G around 400–460 °C, R_H had a stable positive sign. For these, we extracted mobilities in the regime $\mu = 0.01$–0.06 $cm^2/(Vs)$, and carrier concentrations in the range of $p = (0.5 - 2) \times 10^{21}$ cm^{-3}. Low mobilities are unfortunately a common drawback of many p-TSOs[15] as Table I reveals.

To corroborate the majority charge carrier type, we performed scanning capacitance microscopy (SCM) measurements using a PARK Systems XE-150 scanning probe microscope. In SCM, a dc-bias modulated with an ac-bias is applied between the sample and the Pt/Ti probe of the instrument. The capacitance-voltage (*C*–*V*) relation of the locally formed metal-insulator-semiconductor structure or Schottky contact between probe and sample is then used to generate SCM signals. For the determination of the type of majority carriers, one uses the fact that the *C*–*V* curves between probe and p- or n-type semiconductor exhibit opposite slopes.[16] Identical ac-voltage variation then leads to capacitance variation, but with opposite phase. Thus, a change of 180° in the SCM phase signal corresponds to a change of majority carrier type.

To scan along a ZnO/ZCO junction, we first deposited a ZCO thin film on an *a*-sapphire substrate at

[a]Author to whom correspondence should be addressed. Electronic mail: fschein@rz.uni-leipzig.de
[b]Also at Laser Zentrum Hannover e.V., Hollerithallee 8, 30419 Hannover, Germany.

TABLE I. Properties of fully or half amorphous (semi)transparent oxide pn heterojunctions as reported in various publications in chronological order. Fabrication methods are abbreviated as: ED: electrodeposition, MS: rf/dc magnetron sputtering, PLD: pulsed-laser deposition, PPD: pulsed plasma deposition, RSPE: reactive solid-phase epitaxy. T_{fab} is the highest used deposition or annealing temperature and RT means room temperature. Optical transmittance T_{VIS} in the visible spectral range (wavelength of 400–800 nm) is listed for entire device or p-layer only.

p,*n*-material	Method	T_{fab}(°C)	Substrate	Amorphous	p, n (cm^{-3})	σ (S/cm)	μ (cm^2/(V s))	T_{VIS} (%)	I_f/I_r	η	Ref.
$ZnRh_2O_4$	MS	RT	Glass	Yes	4.2×10^{16}	2		40 (at 555 nm)	1000 (±4 V)	2.3	10
InGaZnO	MS	RT		Yes							
$CuAlO_2$	PLD	400	Glass	Yes		0.1		43 (at 500 nm)	90 (±1.5 V)		4
ZnO	PLD	350									
LaCuOSe	RSPE		MgO		1×10^{19}		8		10 (± 8 V)		18
InGaZnO	PLD	RT		Yes	1×10^{19}						
$ZnCo_2O_4$	PLD	RT	AL_2O_3	Yes	2×10^{17}	33	1		100 (± 7 V)		5
InGaZnO	MS	RT		Yes	1.8×10^{17}						
$Ni_{0.9}Cu_{0.1}O$	PPD	RT	Glass	Yes	4.2×10^{18}	0.2	0.3	53	90 (± 3 V)		19
In_2O_3:W	MS	RT			1.1×10^{18}						
NiO	ED	150	Glass	Yes				75	3000 (± 1 V)		20
ZnO	ED	150									
SnO	MS		Glass	(Yes)[a]	1×10^{19}		<1.2	15	12 (±4.5 V)	11.2	21
ZnO	MS										
$ZnCo_2O_4$	PLD	RT	AL_2O_3	Yes			<0.06	65	2×10^{10} (±2 V)	2.04	This work
ZnO	PLD	650									

[a]Depends on not specified annealing temperature used for the diode.

$p(O_2) = 0.016$ millibar and $T_G = 460$ °C followed by a ZnO thin film grown at 0.02 millibar and the same temperature. Usually, our ZnO thin films are grown at an optimized higher temperature of 650 °C. However, ZCO films grown at 650 °C exhibited a drop in conductivity by a factor of 1000 together with the appearance of a ZnO phase as observed in XRD. Starting deposition with a ZnO thin film in order to avoid high temperature exposure of the ZCO film was not an option because we were not able to wet etch ZCO. Therefore, T_G of ZnO was reduced to 460 °C. Then, we took advantage of selective etching and removed laterally half of the ZnO film using diluted phosphoric acid. Figure 1 shows a

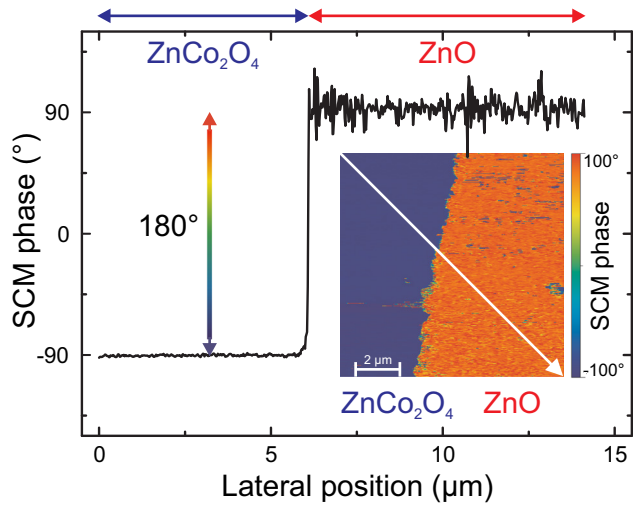

FIG. 1. $5 \times 5\,\mu m^2$ scanning capacitance microscopy phase image of $ZnCo_2O_4$/ZnO interfacial region (inset) and phase signal along diagonal linescan (white arrow in inset). Phase shift of 180° proves opposite type of majority carriers.

SCM phase scan along the ZnO/ZCO edge of this sample. The 180° jump in SCM phase proves opposite charge carrier types. Since our ZnO films grown at identical conditions are surely n-type, the ZCO must be p-type.

For the fabrication of n-ZnO/p-ZCO heterodiodes, we used the same growth conditions as for the SCM sample, but an additional Al-doped ZnO layer on top of ZnO to improve series resistance.[17] Again, selective etching of ZnO allowed to form ZnO pillars of various diameters by means of photolithography. Finally, Au contacts were formed by a second resist mask and subsequent dc-sputtering and checked to be ohmic. The current density vs. voltage (j–V) characteristic of the best diode with this structure is plotted in Fig. 2(a).

We have fitted our diode characteristics numerically according to the (implicit) equation

$$j(V) = j_s \left(\exp\left[\frac{e\,(V - R_s I)}{\eta\, kT} \right] - 1 \right) + \frac{V - R_s I}{A R_p},$$

with R_s (R_p) being the series (parallel) resistance, η being the ideality factor, A being the junction area (here $A = 0.49 \times 10^{-3}\,cm^2$), and j_s being the saturation current density.

The dashed line in Fig. 2(a) represents the good fit with $\eta = 2.59$, $R_s = 14.6\,k\Omega$, $R_p = 8.3 \times 10^7\,\Omega$, and $j_s = 1.5 \times 10^{-6}\,A/cm^2$. As it is obvious from this figure, the reverse current is not due to the saturation current of the diode but to the parallel resistance indicating that either edge currents or shunts limit the rectification of this particular diode. Also $\eta > 2$, which is often observed in wide bandgap heterojunctions,[22] indicates interface imperfections or inhomogeneities.[23] However, despite promising results, the yield of such ZnO on ZCO diodes grown at 460 °C was poor.

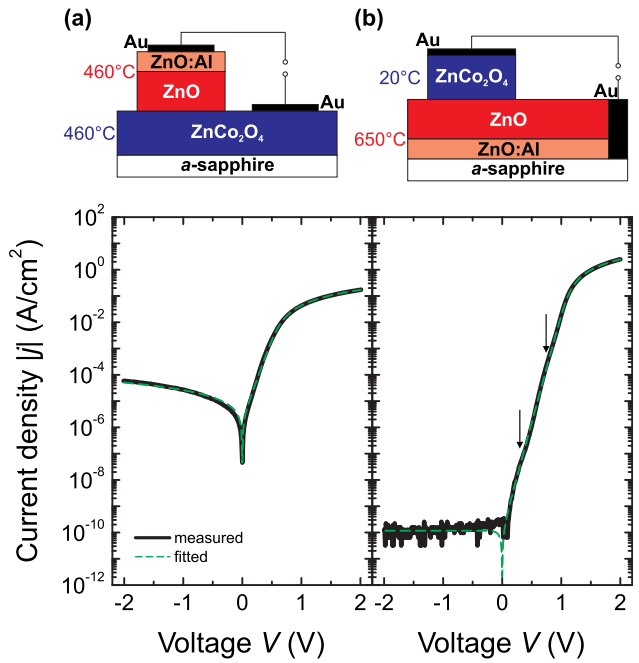

FIG. 2. Sketches of (a) ZnO/ZCO or (b) ZCO/ZnO diode structure and corresponding measured (straight) and fitted (dashed) *j–V* characteristics of highest rectifying diodes. Growth temperatures of respective oxide films are labeled. Arrows in (b) indicate slight kinks which are due to small interface regions with lower barrier.

Therefore, we developed an inverted diode structure. As a starting point, optimized conditions of 650 °C and 0.016 millibar were applied for the ZnO:Al and ZnO layers. The ZCO layer was then deposited at room temperature for several reasons. First, the usage of amorphous films is a first step towards flexible, room temperature fabricated devices. Second, these films were also p-type conductive as revealed by Seebeck effect measurements at Helmholtz-Zentrum Berlin. Using a mean temperature of 65 °C and $\Delta T = 8$ °C, we found positive Seebeck-coefficients S for all samples and values between $S = +240$ and $+300\,\mu$V/K for most of them. Finally, it was possible to pattern the ZCO in advance via photolithography without chemical wet etching. Otherwise elevated ZCO growth temperatures would damage the photoresist. Circular contacts with diameters of 150–750 µm were defined by a resist mask before ZCO deposition. After the growth of ZCO, ohmic Au contacts were dc-sputtered using the same mask. Finally, lift-off was carried out. The complete device structure is depicted at the top of Fig. 2(b). The oxygen partial pressure during ZCO deposition turned out to have minor influence on diode characteristics if $p(O_2)$ is within 0.03–0.1 millibar. In this pressure regime, measurements of ZCO films on glass revealed increasing transmittance from $T_{VIS} = 30\%$ to 64%, and decreasing conductivity from 1.6 to 0.0003 S/cm when $p(O_2)$ rises. Table I points out that these values are comparable to those of other materials used for oxide pn-diodes.

Figure 2(b) shows the *j–V* characteristic of the ZCO/ZnO diode with highest rectification. Here, $p(O_2)$ during ZCO deposition was 0.1 millibar. The ratio of forward to reverse current $I_f/I_r = 2 \times 10^{10}$ at $\pm$ 2 V far exceeds values of similar (semi)transparent oxide heterojunctions comprising at least one amorphous material. Such devices are compared in Table I. The rectification ratios of other reported diodes are below 3×10^3. Also the ideality factor of $\eta = 2.04$ obtained from a fit represents the best (smallest) value within this comparison. Further fit parameters were $R_s = 969\ \Omega$ and $j_s = 1.2 \times 10^{-10}$ A/cm² ($A = 0.31 \times 10^{-3}$ cm²). A significant R_p could not be determined due to the constant reverse current behavior. The improvement compared to the prior diode attempt is obvious. However, a comparison of experimental and calculated data reveals two small kinks in the forward current. These are due to comparatively small regions of the interface area in which the built-in potential is reduced. Hence, these regions are under flat band conditions already for smaller voltages than the main part of the diode. This multiple barrier phenomenon was described in more detail by Müller *et al.*[23] for ZnO Schottky diodes.

The *j–V* characteristics of a typical ZCO/ZnO diode is plotted in Fig. 3(a) ($p(O_2)(ZCO) = 0.03$ millibar). Here, the dark blue curve represents a measurement directly after device fabrication. The light blue line in the same plot stems from the same contact measured more than 1 year (393 days) later. During this rather long time period, the characteristics has changed only little. The mean η obtained from fitting 34 individual diodes on this sample even improved from 2.07 to 1.98. Single devices exhibit η around 1.7 as histograms of the data reveal (Fig. 3(b)). The mean R_s changed from 520 Ω to 1848 Ω, resulting in a decrease of mean rectification from 7.0 to 6.4 orders of magnitude. Reasons for a decrease of R_s are not clear yet, but besides changes within the ZCO changes of the ZnO layer or the ZnO:Al back contact are likely. Indications for the long-term stability were already demonstrated by the bias stress stability of our junction-field effect transistors.[11]

In summary, we investigated $ZnCo_2O_4$ as p-type layer in oxide heterojunctions. ZCO thin films fabricated at certain conditions showed p-type conductivity in Hall effect which

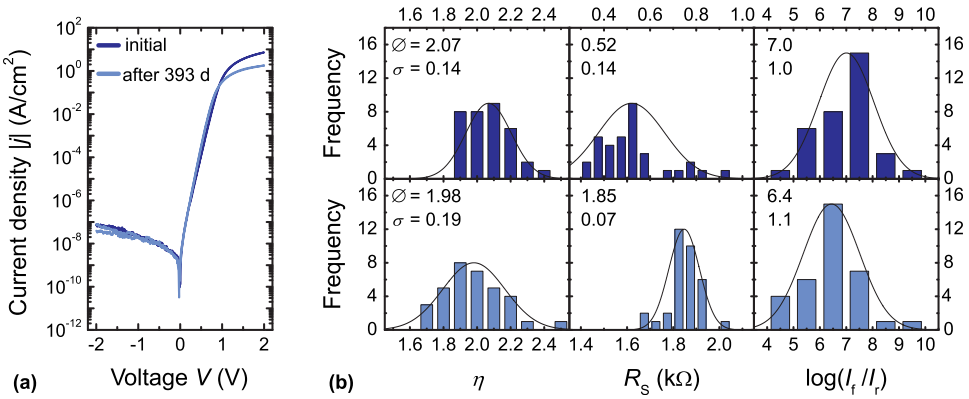

FIG. 3. (a) Typical ZCO/ZnO *j–V* characteristics measured shortly after fabrication (dark blue) and more than one year later (light blue). (b) Histograms of fit parameters ideality factor η and series resistance R_s obtained from 34 individual diodes as well as logarithm of current rectification ratio. Top (bottom) row corresponds to initial (later) measurements. Respective mean value ∅ and standard deviation σ are labeled in upper left corner.

was additionally verified by scanning capacitance microscopy. Seebeck effect measurements confirmed this charge carrier type also for other PLD parameters, especially for amorphous ZCO films deposited at room temperature. First attempts of n-ZnO/p-ZCO diodes prepared at 460 °C revealed rectifying contacts, having $I_f/I_r = 4300$ and $\eta = 2.6$. Improved diodes using room temperature deposited ZCO on epitaxial ZnO/Al_2O_3 resulted in rectification ratios up to 2×10^{10} and $\eta = 2$. Furthermore, the diode long-term stability exceeds one year. The promising results encourage substitution of crystalline ZnO to pave the way towards fully amorphous oxide diodes with high rectification.

This work was funded by Deutsche Forschungsgemeinschaft in the framework of Sonderforschungsbereich 762 "Functionality of Oxide Interfaces".

The authors thank G. Ramm for PLD target fabrication, H. Hochmuth for growing the thin films, M. Hahn for assistance in photolithography, C. Kranert for Raman spectroscopy, V. Zviagin for language editing, and especially D. Splith for providing fit-software tools; all Universität Leipzig. We gratefully acknowledge A. Bikowski and K. Ellmer from Helmholtz-Zentrum Berlin for support in Seebeck-coefficient measurements.

[1]*Transparent Conductive Zinc Oxide*, Springer Series in Materials Science, edited by K. Ellmer, A. Klein, and B. Rech (Springer, 2008).
[2]*Functional Oxides, Inorganic Materials*, edited by D. W. Bruce, D. O'Hare, and R. I. Walton (John Wiley & Sons, Ltd, 2010).
[3]N. Münzenrieder, C. Zysset, L. Petti, T. Kinkeldei, G. A. Salvatore, and G. Tröster, Solid-State Electron. **87**, 17 (2013).
[4]K. Tonooka, H. Bando, and Y. Aiura, Thin Solid Films **445**, 327 (2003).
[5]S. Kim, J. A. Cianfrone, P. Sadik, K.-W. Kim, M. Ivill, and D. P. Norton, J. Appl. Phys. **107**, 103538 (2010).
[6]H. Mizoguchi, M. Hirano, S. Fujitsu, T. Takeuchi, K. Ueda, and H. Hosono, Appl. Phys. Lett. **80**, 1207 (2002).
[7]T. R. Paudel, A. Zakutayev, S. Lany, M. d'Avezac, and A. Zunger, Adv. Funct. Mater. **21**, 4493 (2011).
[8]J. D. Perkins, T. R. Paudel, A. Zakutayev, P. F. Ndione, P. A. Parilla, D. L. Young, S. Lany, D. S. Ginley, A. Zunger, N. H. Perry, Y. Tang, M. Grayson, T. O. Mason, J. S. Bettinger, Y. Shi, and M. F. Toney, Phys. Rev. B **84**, 205207 (2011).
[9]P. F. Ndione, Y. Shi, V. Stevanovic, S. Lany, A. Zakutayev, P. A. Parilla, J. D. Perkins, J. J. Berry, D. S. Ginley, and M. F. Toney, "Control of the Electrical Properties in Spinel Oxides by Manipulating the Cation Disorder," Adv. Funct. Mater. (published online).
[10]S. Narushima, H. Mizoguchi, K. Shimizu, K. Ueda, H. Ohta, M. Hirano, T. Kamiya, and H. Hosono, Adv. Mater. **15**, 1409 (2003).
[11]F.-L. Schein, H. von Wenckstern, H. Frenzel, and M. Grundmann, IEEE Electron Device Lett. **33**, 676 (2012).
[12]F. Klüpfel, F.-L. Schein, M. Lorenz, H. Frenzel, H. von Wenckstern, and M. Grundmann, IEEE Trans. Electron Devices **60**, 1828 (2013).
[13]H. J. Kim, I. C. Song, J. H. Sim, H. Kim, D. Kim, Y. E. Ihm, and W. K. Choo, J. Appl. Phys. **95**, 7387 (2004).
[14]A. Zakutayev, J. Perkins, P. Parilla, N. Widjonarko, A. Sigdel, J. Berry, and D. Ginley, MRS Commun. **1**, 23 (2011).
[15]G. Hautier, A. Miglio, G. Ceder, G.-M. Rignanese, and X. Gonze, Nat. Commun. **4**, 2292 (2013).
[16]A. Krtschil, A. Dadgar, N. Oleynik, J. Bläsing, A. Diez, and A. Krost, Appl. Phys. Lett. **87**, 262105 (2005).
[17]H. von Wenckstern, G. Biehne, R. A. Rahman, H. Hochmuth, M. Lorenz, and M. Grundmann, Appl. Phys. Lett. **88**, 092102 (2006).
[18]H. Hiramatsu, K. Ueda, H. Ohta, T. Kamiya, M. Hirano, and H. Hosono, Appl. Phys. Lett. **87**, 211107 (2005).
[19]M. Yang, Z. Shi, J. Feng, H. Pu, G. Li, J. Zhou, and Q. Zhang, Thin Solid Films **519**, 3021 (2011).
[20]E. Azaceta, S. Chavhan, P. Rossi, M. Paderi, S. Fantini, M. Ungureanu, O. Miguel, H.-J. Grande, and R. Tena-Zaera, Electrochim. Acta **71**, 39 (2012).
[21]K. Sanal and M. Jayaraj, Mater. Sci. Eng., B **178**, 816 (2013).
[22]M. Brötzmann, U. Vetter, and H. Hofsäss, J. Appl. Phys. **106**, 063704 (2009).
[23]S. Müller, H. von Wenckstern, O. Breitenstein, J. Lenzner, and M. Grundmann, IEEE Trans. Electron Devices **59**, 536 (2012).